Third United Nations International Conference on the Peaceful Uses of Atomic Energy

A/CONF.28/P/317
USSR
May 1964
Original: RUSSIAN

Confidential until official release during Conference

THEORETICAL AND EXPERIMENTAL INVESTIGATIONS CONNECTED WITH DEVELOPMENT OF THERMIONIC REACTOR – CONVERTERS.

I.I. Bondarenko, I.N. Gorelov, Yu.K. Gus'kov, V.M. Dmitriev, I.I. Kasikov, V.P. Karmasin, S.Ya. Lebedev, M.A. Lebedev, V.A. Malikh, S.A. Majev, V.Ya. Pupko, V.G. Petrovskii, V.P. Paschenko, E.E. Sibir, Y.Ya. Stavisskii, I.P. Stakhanov, A.S. Stepanov, Yu.S. Yur'ev.

The direct conversion of heat into electric energy has some essential advantages in comparison with machine conversion. It makes possible to avoid travelling parts, to increase the efficiency of an electric plant (in particular for combination of the unmachine converter with an ordinary electric generator), to enlarge the specific power of an electric plant in some applications. Three conversion methods are of the greatest interest: thermoelectric, thermionic and magnetohydrodynamic ones.

The first method, connected with the application of semiconductor thermoelements, is profitable in the case of comparatively small powers (10–100 kw). On the contrary, the use of MHD generators is expedient in plants of a great power ($10^5 - 10^6$ kw). The thermionic method of the conversion with electron gas as a working body has significant advantages in the range of middle powers. The thermionic principle of the heat-into-electricity conversion is convenient to be used in a device with a nuclear reactor as a source of heat.

The results of the theoretical and experimental investigations connected with the design of a thermionic reactor-converter are presented in this report.

The many works have been devoted to the investigations of thermionic conversion [1 – 6]. In the early works the utilization of the difference between the cathode and anode work functions in vacuum was proposed. To decrease the influence of a space charge limiting the current in a vacuum converter it is necessary to reduce the spacing between electrodes to approximately 10μ. It was later proposed to inject the vapour of cesium into the interelectrode spacing; its ionisation allows to increase the interelectrode spacing to practically acceptable sizes (~1mm). In this case the interelectron spacing is filled by cold plasma.

1. CONVERTER WITH LOW PRESSURE OF CESIUM VAPOUR.

It is known that the injection of even very small amount of cesium vapours ($10^{-3} - 10^{-4}$ mm Hg) permits to neutralize completely the space charge of electrons in the interelectrode space (the quasivacuum regime). In this regime the current is limited by the emission capabilities of the cathode and therefore the great currents can be obtained either

at high temperatures (T >2500°K) or when low work function cathodes are used which can work in reactor for a long time. In particular one can use a fall of the work function due to the adsorption of cesium atoms on the surface of refractory metals.

The investigations of thermoemission parameters of some refractory metals (Zr, Hf, Nb, Ta, Ti, Mo, C, W, Ni, Re) in the cesium vapours have been carried out.

The work functions Wo and specific evaporation heats of cesium Qo for optimum surface covering calculated from the total current are summarized in Table I (W is the work function of the cathode without cesium covering). From the Table it is seen that the work function and evaporation heat of cesium at optimum covering increases linearly with the work function of the cathode material for majority of metals. It should be noted that rather large cesium pressure is required for obtaining of the optimum work function.

The quasi-vacuum regime was investigated in a number of works. In these conditions the scattering of electrons on the neutral cesium atoms can be neglected so the corresponding free path is considerable larger than interelectrode spacing. The coulomb scattering, however, can be imported even at very low pressure if the ionisation degree is significant.

2. CONVERTER WITH HIGH PRESSURE OF CESIUM VAPOUR.

2.1. The cathode work function decreases with increasing of cesium vapour pressure. As a result the power of the converter increases with pressure. However, at the same time the electron scattering on atoms becomes more important limiting eventually the growth of current and power. At high pressure the ionisation of cesium atoms in the volume begins also.

At pressure p≃1 mm Hg the mean free path for the electron scattering on atoms (l_e) appears to be much less than the interelectrode spacing (L). We call it "diffusion regime". For cathodes covered by cesium the power maximum corresponds to this very regime. The role of the volume ionisation and conditions of its arising will be examined in the next section. In the present section the ionisation on the cathode surface is assumed to predominate.

A voltage-current characteristic in a diffusion regime with the cathode ionisation has the saturation current (I_s) which, however, is usually much less than the electron emission current: at L=1mm and T=1500°K I_s=1a/cm^2. The value of I_s (unlike the quasi-vacuum regime) depends essentially on the interelectrode spacing. In addition, I_s as well as the output voltage does not depend on the cathode material in wide interval of temperatures and pressure and is determined by the cathode temperature (T') and cesium pressure (P) only [12]. An electron temperature (T_e) can differ essentially from that of atoms (T) due to the fact that energy exchange between electrons and atoms is hindered. In particular at low currents ($I \ll I_s$) an electric field in the interelectrode spacing moderates the electrons cooling the electron gas. On the contrary at high currents ($I \simeq I_s$) the accelerating field arises which heats the electrons. The temperatures of heavy particles (ions and atoms) are always practically equal. The ionisation degree in the conditions under consideration is small (0.1% or less). However, for the pressures less than 1 mm Hg and for high temperatures (T' 2000°K) the ionisation degree increases appreciably and the coulomb scattering dominates 10.

2.2. The diffusion fluxes of electrons (I) and ions (i) as well as the electron energy flux (Q) are given by:

$$I = -D_e \, dn/dx + U_e \eta \, d\phi/dx - D_e^T \, dTe/dx$$
$$j = -D_i \, dn/dx - U_i \eta \, d\phi/dx - D_i^T \, dTe/dx \qquad (1)$$
$$Q = -\lambda_e \, dTe/dx + I(\varkappa T_e - e\phi)$$

where $D_{e,i}$; $U_{e,i} = \frac{eD_{e,i}}{kT_{e,i}}$; $D_{e,i}^T$ are the electron and ion coefficients of diffusion, mobility and thermodiffusion, respectively, λ_e is the thermal conduction coefficient, $\varkappa$ is the "heat of transfer" for electrons, ϕ is the potential, η is the plasma density. The kinetic coefficients in Eq.(1) for a three component plasma (electrons, ions and atoms) in arbitrary magnetic field have been calculated by the Chapman-Enskog method [11]. In this work both the collisions with the neutral atoms and the coulomb scattering are taken into account. The latter was taken into account by adding the collisional term in the Landau form in the kinetic equation. If there is no volume ionisation:

$$\frac{dI}{dx} = 0; \qquad \frac{dj}{dx} = 0; \qquad \frac{dQ}{dx} = 0 \qquad (2)$$

The value of the saturation current I_s is given accurately enough by expression (see [12]):

$$I_s = (1+\frac{T_i}{T_e}) \frac{\eta'}{L} D_e = (1+\frac{T_i}{T_e}) \frac{1}{3} \eta' \bar{v}_e \frac{le}{L} \qquad (3)$$

where $\bar{v}_e$ is the average thermal velocity of electrons, η' is plasma density at the cathode, le, L are the mean free path of electrons and interelectrode spacing respectively. The description of the iteration method applied to an accurate numeral solution of the set of Eqs (1), (2) is given in [14]. For plane geometry in the absence of the coulomb collisions the potential can be shown to depend logarithmically on the distance and the density decreases linearly towards the anode. The results of numeral calculations of voltage-current characteristics agree well with the experiment if the electron scattering-cross-section is $(1-2)\cdot 10^{-14}$ cm^2 [13, 14].

2.3. The boundary conditions for Eq. (2) can be obtained from the conservation laws for the particle number and energy in the layer near electrode [14], [12]. The main parameter characterizing the boundary conditions at cathode is compensation parameter ω:

$$\omega = \frac{j_o}{I_o}\sqrt{\frac{M}{m}} \qquad (4)$$

where I_o, j_o are the electron and ion emission currents from cathode; m, M are the electron and ion masses. At $\omega>1$ we call the operation regime by "overcompensated" one. In this case the chemical potential of plasma is less than the cathode work function. The potential jump arises which reflects the surplus ion emission: $\Delta\phi'>0$ (see Fig.1). At $\omega<1$ (the "undercompensated" regime) the plasma potential is less than the cathode potential:

If ω is about unity so that $(\frac{l}{L})^2 \ll \omega \ll (\frac{L}{l})^2$ the local thermal equilibrium takes place on the boundary and thus the density η' can evaluate from Saha's equation. At $\omega<1$ the density near cathode is given by the following expression [15]:

$$\eta' = \eta_o\sqrt{1-j/j_o} \qquad (5)$$

where η_0 is the equilibrium density determined from Saha's equation. From the Eq. (5) it is seen that in the saturation current regime, i.e. when $j = 0$:

$$\eta' = \eta_0$$

Thus in a undercompensated regime the saturation current value, Eq. (3), is determined by the equilibrium density too. If the electron heating in the potential barrier near the electrode is not taken into account we shall obtain for the overcompensated regime [15]:

$$\eta' = \eta_0 \sqrt{1 - I/I_0} \qquad (6)$$

which results in $\eta' < \eta_0$ and consequently at $\omega > 1$ I_s is less than for the equilibrium regime (at the same temperature and pressure). By using Eqs (3) and (6) it is easy to show that $I_s \to I_0$ at $\omega >> (L/l)^2$. The typical results of the computation of the voltage current characteristics for various values of the cathode work function are given in Fig.2. It is seen that in the undercompensated regime ($W' < 2.8$ev) the change of the work function (W') practically does not effect on the voltage-current characteristic. On the other hand, even the relatively small overcompensation ($W' > 2.8$ev) results in considerable decreasing of the current. That follows also from Fig.3 where the computed saturation current and power (P) are plotted versus the cathode work function. With further decreasing of the cathode work function i_s and P decrease also (for example because of the ion recombination). The experiment confirms these conclusions. So, the typical curve of the short-circuit current (which practically equals I_s) is given in Figs 4-5. It is seen from these curves that at low temperatures ("ab") which correspond to the undercompensated regimes the saturation current depends exponentially on the temperature, exponent equalling to half of the cesium ionisation energy as it should be for the equilibrium density near the cathode. At further temperature increasing the regime turns into overcompensated one and the rate of the current increasing drops with the temperature increasing ("bc"). This occurs at the temperatures as large as pressure and the cesium adsorption energy on a cathode greater. Using the data obtained and formulae (6) and (3) one can compute the cathode emission current and determine its work function. The results of this calculations are given in Fig. (6). They are in good agreement with the data obtained in reference [17].

2.4. The special interest is to consider the intermediate pressure region between the diffusion and quasi-vacuum regimes. Some conclusions about plasma behaviour in these conditions can be obtained by solving of the kinetic equation by the expanding of the distribution function into series of complete orthogonal function sets. In particular, the method of symmetrized Hermit polynomial expansion was applied. Thus the relation between the saturation current I_s and the ratio of a mean free path to the system's dimension ($K = \frac{le}{L}$) was obtained. For the undercompensated regime we have [19]:

$$I_s = \frac{1.73 K}{(1.5\alpha^2 K^2 + 2.6\alpha K + 1)^{1/2}} \sqrt{\omega I_0} \qquad (7)$$

where α is factor of the order of unity ($10/9 < \alpha < 21/16$) depending on the electrodes and plasma temperatures only. It is seen from Eq.(7) that at low pressure ($K \to \infty$) I_s does not depend on K (i.e., on pressure and system's dimension). In this case I_s can be shown to coincide with that

part of saturation current which passes through the barrier near cathode ($\Delta\phi' < 0$):

$$I_s = I_0 \exp\left(e\Delta\phi'/kT\right) \qquad (8)$$

On the contrary, at large pressure we have:

$$I_s = 1.73\alpha K \sqrt{\omega} I_0 \qquad (9)$$

Since $\sqrt{\omega} I_0 = \frac{1}{4} \eta_0 \bar{v}_e$, Eq.(9) coincides with Eq.(3) given above for the diffusion regime.

Further one can obtain more precise boundary conditions, in particular, for the connection between the particle flux on the wall (I) and plasma density near the wall (η'). On the boundary with cold wall in absence of moderating potential jump we have [20]:

$$I = \frac{1}{2} \eta \bar{v} \left(1 + \frac{P_{xx}}{P}\right) \qquad (10)$$

where P is plasma hydrostatic pressure, P_{xx} is stress viscous tensor (the x axis is normal to the wall), $\bar{v} = \sqrt{8kT/\pi m}$ is average thermal velocity. Neglecting by the small value of P_{xx}/p we obtain $I \simeq \frac{1}{2} \eta \bar{v}$ instead of the usual relation $I = \frac{1}{4} \eta \bar{v}$. If the emitting wall and potential jump are in presence the appropriate expressions are more complicated.

3. EFFECT OF VOLUME IONISATION.

3.1. The volume ionisation can dominate if the cathode temperature is higher than 1400°K and pressure is high enough. In this case the converter may be considered as working in the conversion regime the lowvoltage arc with heated cathode. The volume ionisation (unlike the surface ionisation) is accompanied by the strong excitation of atoms which results in the noticeable discharge glow. The voltage-current characteristic is entirely different from that for the cathode-ionisation diffusion regime. The rapid current change with voltage, the less value of output voltage and the absence of the saturation current in the conversion region are characteristic.

On the basis of the experimental results obtained one can classify the converter operation regimes and their typical features (Fig.7).

The boundary of the region with essential volume ionisation is determined by the curves II-IV. Here, the type of the process depends on the cathode temperature and cesium vapour pressure. In the region "B" the volume processes result in gradual vanishment of plato on the voltage-current characteristic with the cathode temperature increasing (Figs 8.1 and 8.2). The short-circuit current does not exceed the diffusion-equilibrium current and the temperature of the arc breakdown decrease with the pressure increasing.

In the region "Г" the discharge begins by the sharp current jump and in the voltage-current characteristic the parts with negative resistance appear (Figs 8.3-8.8). In this case the temperature of the arc breakdown increases with pressure. At the operation in the negative resistance part the spherical plasma clouds appear [21]. With the cathode temperature growth the gas glow is extended throughout all the interspace and the negative resistance parts disappear gradually (see Figs 8.5-8.8).

The region of the forced arc breakdown appears because of the discharge voltage-current

characteristics have a hysteresis in a voltage, i.e. the extinction potential of the discharge is generally less than the breakdown potential. In this case the direct and inverse trends of the voltage-current characteristics are shown in Fig. 8.5. The boundaries of the forced arc breakdown region are determined as follows: on the lower boundary the extinction potential equals to zero (curve V in Fig.7); on the upper boundary the breakdown potential equals to zero (curve IV in Fig.7).

Unlike the case of the diffusion regime in the arc regime the short-circuit current depends slightly on the temperature (see Fig.5, "ab") but it depends strongly on the choice of a cathode material. With the variation of temperature from 1800°K to 2200°K the output voltage increases approximately twice.

Owing to the weak dependence of the current upon a temperature, at the temperature high enough (the region "B") the lowvoltage arc regime does not provide a gain in the current and power as compared to the equilibrium diffusion regime. The useful role of the volume ionisation consists in the possibility of obtaining the greater current densities (10-30 a/cm^2 instead of 1-2 a/cm^2) at relatively less temperatures (the region "Г" in Fig.7).

3.2. In the lowvoltage arc the thermal ionisation dominates, i.e. the ionisation is carried out by the fast electrons from the "tail" of the Maxwellian distribution. Therefore the electron gas temperature (T_e) should be considerably larger than the electrode temperatures. The increase of T_e occurs owing to both an electron heating in the barrier near the electrodes and a Joule heating. Therefore the arc starts spontaneously only in the overcompensated regime and the volume ionisation begins near anode where the temperature increasing, caused by a Joule heating, is greatest. The anode glow demonstrates this fact appearing before a discharge. The sharp increasing of the current in the arc regime is probably connected with the anomalous Schottky effect appearing because of the field in the boundary layer between a cathode and plasma. The effects of other processes are also possible (the autothermionic emission, for example).

The mechanism of the volume ionisation of cesium atoms in the arc is still insufficiently studied. The numeral calculations indicate that the ionisation must proceed from the excited states rather than from the ground state. The lifetime of the excited state increases because the plasma absorbs the radiation of the resonance frequencies of cesium atoms.

Let us discuss another effect which may influence the ionisation rate. The beam of electrons accelerated in the charged layer near cathode appears in the "tail" of the distribution function. In the maxwellization process the beam electrons "diffuse" in the momentum space (because the maxwellization occurs through the collisions with small energy transfer); as a result the distribution function enriched by the fast particles appears differing essentially from the Maxwell function at large energies. This effect may lead to the appreciable increase of ionisation rate.

4. EFFECT OF MAGNETIC FIELD ON THERMIONIC CONVERTER OPERATION.

4.1. The elements of the high power thermionic converter are to be placed in magnetic field (100 oersted or more) of current-carrying electrodes. Therefore the effect of magnetic field on the converter operation is of practical interest [23]. The influence of transverse field on the

diffusion regime current is illustrated by the curve in Fig.9 [10]. The current decrease is explained by the decrease of the electron diffusion coefficient (see Eq.3):

$$D_e(H) = \frac{D_e(0)}{1 + \Omega^2 \tau^2 f(H)} \qquad (11)$$

where $\Omega = \frac{eH}{mc}$ is cyclotron frequency, H is magnetic field, f(H) is a certain fractional-linear function determined by the kinetic theory, τ is the time of the electron free flight. It should be noted that the appreciable deviation of the ordinary curve form is observed at large magnetic fields (H>100 oersted), the strong oscillations being generated in plasma. These deviations are probably connected with the anomalous plasma diffusion in magnetic field.

Near an electrode the density variation with application of magnetic field should be taken into account for the correct estimate of the magnetic field effect. By writing the laws of conservation of particle number and energy in the layer near electrode whose thickness is of the order of mean free path, this effect may be estimated. The distribution functions of particles entering into the layer from a wall or from plasma can be given as Maxwell functions with appropriate temperatures. In the layer the particles move without collisions, the electrons being deflected by magnetic field. The electrons emitted from a wall or from plasma with small value of the velocity normal component are turned by magnetic field leading to the formation of the reflected flux.

Since the thickness (δ) of the charged layer near electrode is essentially less than the free path (l_e) the electric field effect is important only in the narrow boundary region, i.e.

$$R = \frac{mcv_e}{eH} \simeq l_e >> \delta$$

The assumptions made allow to find the ion and electron distribution functions with the help of which the conservation laws of particle number and energy can be written. The solution of this equation allows to determine the plasma density, the potential jump and the electron temperature near the electrodes.

At $\omega<1$ the plasma boundary density depends only on the H/p (P is pressure) and decreases with increasing of H; the effect of magnetic field is weak (the correction terms are of the order of $\frac{l_e}{L}$). At $\omega>1$ the effect of magnetic field is stronger, the density being increased with magnetic field.

A physical reason for the increase of density is following. When magnetic field is applied the electron current from the boundary layer into plasma is appreciably decreased, it being determined by the particles with the average thermal velocity. At the same time magnetic field almost does not effect on the electron flux from a wall into the boundary layer, the latter being determined by the fast particles accelerated in the charged layer. As a result the plasma density increases near the cathode. At $\omega<1$ it is evident that similar situation does not exist.

At $\omega>1$ owing to the growth of the boundary density the current decreases more slowly with increase of magnetic field in comparison with the diffusion coefficient and may even increase

slightly in weak fields. In Fig. 10 the calculated voltage-current characteristics for some magnetic fields are given.

4.2. It should be noted that in the volume ionisation regime the longitudinal magnetic field (along the current direction) effects essentially the low-voltage arc. This effect is illustrated by the curve in Fig. 11. The data given in this figure are obtained at the low cathode temperature (1100°K) under applied external voltage. From Fig. 11 it is seen that at $l \ll L$ (curves 3-5) the monotonous current decrease with the growth of magnetic field is observed which can lead even to a current cutting off. This phenomenon can be explained as follows. As it was noted above, in the low-voltage arc the potential maximum is observed between the electrodes. The appreciable part of slow electrons generated due to ionisation in the maximum potential region is gone from the interelectrode space into the chamber walls because of the ambipolar diffusion. In magnetic field the electron diffusion in transverse direction decreases while the positive ions keep to diffuse towards the chamber walls. This leads to an increase of the slow electron concentration inside the discharge space and to a partial filling of the potential well. The well depth decreases to restore the ambipolar diffusion into the wall. The decrease of the well depth with increasing of H implies the decrease of the potential near the cathode and, consequently, the fall of the electron temperature. This results in the decrease of an arc current down to a discharge cutting off. The current increase at $l \gg L$ (Fig. 11, curve I) can be explained by the increasing of ionisation efficiency due to the fact the electrons emitted at small angles from a cathode surface are turned by magnetic field.

5. THE CURRENT OSCILLATION IN THE THERMIONIC CONVERTER

The study of the oscillations in the thermionic converter is of certain interest not only for physical investigations but the industrial utilization too, for example, as the energy source for radio-communication or for conversion of a low-voltage direct current into an alternating current.

The oscillations have been observed, at first, in the range of the high temperatures ($T' > 1900$°K) and low pressure ($P \lesssim 5 \cdot 10^{-2}$ mm Hg), and second at the low temperatures ($1200° \leqslant T' \leqslant 1500$°K) and high pressure ($0.04 \leqslant P \leqslant 0.6$ mm Hg) [16]. The oscillation frequency varies between a few kilocycles and a few megacycles depending on the conditions. It the should be noted that in the latter range the collisions with neutral atoms are important and in the former the coulomb scattering is important. The explanation of the origin of these oscillations (see [18]) seems to be not adequate since it is not shown how the ion cloud is formed and exists in spite of scattering. In addition, the oscillations are observed even though the potential has not a form of the ion catcher. The oscillations are possibly connected with the plasma beam instability in the region near cathode. Though the distribution function near the cathode is almost Maxwellian one it seems to differ significantly from the ordinary diffusion function. The fact is that in the presence of significant potential jumps on boundaries the disturbances of the distribution function near the boundaries are localized in high energy range. At $\omega > 1$ these disturbances are formed by the beam of the emission electrons accelerated in the charged boundary layer near the cathode. At $\omega < 1$ the analogous ion beam appears. The presence of the beams is the cause of arising of the beam instability and it can be shown that

317

the increment of the long wave oscillations is:

$$I_m\frac{\omega}{k} = \frac{V}{1+\beta^2}\,\beta\sqrt{1-\frac{1+\beta^2}{\beta^2}\,(\eta^2+\beta^2)\,\frac{C_1^2}{V^2}} \qquad (12)$$

where ω is a frequency, k is a wave vector, β is a ratio of the beam density to the density of motionless plasma, $C_1=\sqrt{\frac{Te}{m}}$, ηC_1 are dispersions of thermal velocities in plasma and in beam, V is an average beam velocity. From the above equation the increment is seen to be real if the beam velocity V is large enough. At this condition the random long wave disturbances appearing near an electrode will spontaneously grow with time.

It can be shown that the oscillations of a current and a potential on the boundary are connected in the following way:

$$\frac{\delta I}{I} = \frac{1-{}^{I}/_{I_0}}{{}^{I}/_{I_0}}\;\frac{e\delta\phi}{kTi}\,(1+\frac{Ti}{Te}) \qquad (13)$$

where I is an average value of the current through the converter. The oscillations of potential, current and density at the boundary will cause the similar oscillations in the volume where the collisions influence on its propagation essentially.

Considering the propagation of the small perturbations of n and ϕ the following dispersion equation can be obtained by means of the linearization of the diffusion equation:

$$\frac{\omega}{k} = \sqrt{\frac{Te+Ti}{M}}\sqrt{\frac{\omega\tau_2}{\omega\tau_2+i}} \qquad (14)$$

where τ_2 is time of the ion free flight between collisions. From the Eq. (14) it follows that the oscillations appeared on boundaries will damp in plasma on the given distance the stronger the less wave-length is. It should be noted that the propagation velocity of those oscillations is determined by the thermal ion velocity ($\sqrt{(Te+Ti)/M}$).

After going through plasma the oscillations appear into a circuit and through a cathode afresh in plasma. Thus, for amplification of the oscillations the whole number of waves should be placed between anode and cathode. From the condition of resonance for first harmonic of the longest wave we find the expression for the oscillation frequency:

$$f=2\pi\omega=\frac{1}{2}\pi^2(1+\frac{Te}{Ti})\frac{l_i}{L}\frac{v_i}{L}\;\frac{1}{\sqrt{1+2\pi^3(l_i/L)^2(1+Te/Ti)}} \qquad (15)$$

From Eq. (12) it follows that the oscillations should be observed at the value of the beam velocity V great enough, i.e. at a positive jump $\Delta\phi$' great enough. This agrees with the fact that oscillations in a diffusion region are observed in the overcompensated regime. At the very great overcompensations the oscillations disappear again. Indeed in this condition $I\to I_0$ and, thus, according to Eq. (13) $\delta I\to 0$. The absence of the oscillations in the undercompensated regime at $I\to I_0$ is explained by the disappearance of the ion current, i.e. of the ion beam exciting

instability in these conditions. The oscillations connected with instability of the ion beam can be probably detected in undercompensated regime in a "tail" of the voltage-current characteristics.

At high pressure when the second term under the square root in Eq. (15) can be neglected the oscillation frequency is inversely proportional to the square of distance:

$$f = \frac{1}{2}\pi^2\left(1+\frac{Te}{Ti}\right)\frac{l_i v_i}{L^2}$$

On the contrary at low pressure the frequency is inversely proportional to the distance:

$$f = \frac{1}{2}\sqrt{\frac{\pi}{2}}\sqrt{1+\frac{Te}{Ti}}\;\frac{v_i}{L}$$

This agrees with the published experimental data. The frequencies calculated from Eq. (15) are in good agreement with the results of the measurements [9, 16, 18].

6. OPERATION OF THE THERMIONIC CONVERTER IN REACTOR CONDITIONS AND IN LOOP TESTS.

Schematically the thermionic converter as a constituent of the design of a thermionic reactor-converter is presented by a cathode in the form of cylindrical shell in which a heat-producing core is placed. The cathode is surrounded by a cylindrical anode and the space between the anode and the cathode is filled with cesium plasma. A few series-connected elements are put with the layer of electroisolation in the common shell forming a fuel element of the reactor-converter.

The operational conditions of the thermionic converter in reactor effect essentially on its parameters. For example, the nonuniformity of the energy release in a reactor core has the strong effect resulting in the nonuniform heating of the cathodes of different thermionic converters. The energy release density can be essentially flattened in a fast neutron reactor by means of variation of fuel concentration along the core; in thermal neutron reactors it can be made by means of a redistribution of a moderator (the element spacing is increasing from the centre to the periphery). In the thermal reactor by this method almost complete flattening of the energy release can be obtained by varying the volume share of a moderator within 15% with respect to the average value. In the fast neutron reactor the nonuniformity energy release coefficient along radius (K_R) can be reduced to the value 1.1 at a total increase of a loading within 7-10%.

The second cause which has a great effect on the work of the thermionic converter in the reactor conditions is temperature irregularities along the cathode arising due to the heat leaks into the anodes of neighbouring converters through connecting and dividing parts. However, an increase of the commutation heat resistance at the series connection of elements leads to a growth of the ohmic losses. The accounting of these factors (the temperature irregularity along cathode, electric resistance of electrodes and of connecting parts, etc.) allows to construct the voltage-current characteristic of the converter in the

reactor (See Fig.12). In this figure the dotted lines represent the voltage-current characteristics at the constant energy release, the full lines correspond to the isothermal characteristics (at the constant cathode temperature). The admissible regimes of converter operation correspond to the region on the left side of the isothermal characteristic corresponding to the maximum admissible cathode temperature T_{max}(°C). From Fig. 12 it is seen that the output electric power and the overall efficiency of reactor-converter can be increased with increase of the thermal power only to some extent. At too large thermal power the region of the admissible operation regimes is restricted strongly (in the limit case it turns into the short-circuit regime). The maximum power regime is outside of this region and further increase of the thermal power leads to a decreasing of the overall efficiency and output electric power (see Fig.13).

The important stage of the development of reactor-converter consists in transition from the laboratory studies to the investigations of converter operation in reactor conditions (the loop tests). These investigations were carried out in the loop channels of the First Atomic Power Plant and of fast neutron reactor BR-5. It should be noted that the experiments in fast neutron reactors have some advantages from the point of view of calculations of the converter efficiency due to the absence of the neutron self-shielding effects in a converter core. The loop channels were equipped by the close vacuum system, the heavy current terminals, the systems of regulation of anode temperature and the temperature control of the cathode, the anode and other points, the converter characteristic measurement system. The converter was designed as a cylindrical vessel with the cesium thermostat in a lower part; this vessel was connected to the vacuum and other systems ot the loop channel (Fig. 14). The converter fuel element was designed in various versions: as a bare core of the solid solution of UC-ZrC; as a core of UO_2 in the Mo-shell and shells of other materials, with or without emission coverings put on the outside shell surface. The interelectrode distance was 0.4-0.5 mm. The cathode temperature was measured by W-Re thermocouple. The anode temperature was regulated by variation of the composition of the nitrogen-helium gas mixture in the narrow gap between vessel wall and channel wall. In a vacuum channel near the converter vessel the pneumatic valve was placed which allowed to evacuate periodically the converter interelectrode gap during the operation period.

The converter operation in the reactor was investigated at the quasivacuum, diffusion and arc regimes. The temperature distribution along cathode effects strongly on the output converter characteristics. This distribution is determined by a method of the cathode shore and by a commutation passages between cathodes and anodes of neighbouring coverters. In Fig.15 the temperature, current density and e.m.f. distributions are shown for the cathode shored at both ends. The results obtained in these experiments average over some temperature range because of large temperature ununiformity.

In Fig. 16 the calculated and experimental temperatures of the molybdenum cathode are given versus the reactor power for the short-circuit regime (curve 1). Curve 2 illustrates the cathode electron cooling at the current removal corresponding to the optimum load. The typical operation characteristics of the converter in a reactor are shown in Figs 17. and 18, where the voltage-current characteristics and output powers are drawn versus the terminal voltage of the converters with the Mo and UC-ZrC cathodes (the latter was without shell). The output power

317

of the converter with the UC-ZrC cathode versus cesium vapour pressure at various cathode temperatures is shown in Fig. 19. The current oscillations similar to those considered above in section 5 were observed in the reactor experiments.

The closed vacuum system with the pneumatic valve in a loop channel allows to observe both the release of fission products from converter cores and the effect of vacuum and of fission fragments upon a converter operation.

The release of the fission fragments from UO_2 cores was higher than from UC-ZrC ones.

In the vacuum system the solid fragments (e.g., lanthanum) were detected as well as the gaseous fragments.

The converter characteristics in reactor were sufficiently stable at periodic evacuation of the converter interelectrode gap. At work with the closed valve the short-circuit current was appreciably varied, however, after the evacuation of the interelectrode gap the converter parameters were respotted.

The work resource obtained at the loop tests was equal to 320 hours for the converter with UC-ZrC core and 280 hours for the converter with UO_2 core.

Table I

Element	W, ev	Wo, ev	Qo, ev
Hf	3.53	1.73-1.9	3.60
Zr	3.84	1.7-2.0	2.45
Nb	3.98	1.40-1.49	1.3
Ti	4.09	1.39-1.46	1.39
Ta	4.13	1.42-1.48	1.41
Mo	4.24	1.44-1.51	1.52
W	4.52	1.69-1.71	1.89
Ni	4.61	1.86-1.95	1.80
C	4.62	1.69-1.71	1.66
Re	5.04	1.87-1.9	2.03

REFERENCES.

1. *A.F.Ioffe, "Semiconductor Thermoelements", edn. AN USSR, Moscow-Leningrad, 1960.*
2. *A.I. Ansel'm, "Thermionic Vacuum Thermoelement", edn. AN USSR, 1951.*
3. *L.N.Dobretzov, Jurn. Tekhn.Fiz., No.4, 365, (1960).*
4. *N.D.Morgulis, Usp. Fiz. Nauk, 70, 679 (1960).*
5. *W.B.Nottingham, Proc. of 4-th Internat. Conf. on Ionisation Phenomena in Gases, Uppsala, VIII, 1959.*
6. *G.Hatsopulos, Dissertation M.I.I., 1956, Cambridge.*
7. *R.Ya.Kucherov, L.E.Rikenglaz, Jurn.Tekhn.Fiz., 32, 1275 (1962).*
8. *P.L.Auer, H.Hurwitz, J.Appl.Phys., 30, 161 (1959).*
9. *J.Johnson F.M.R.C.A. rev. 22,21 (1960).*
10. *Yu.K.Gus'kov, V.P.Paschenko, I.P.Stakhanov, E.A.Stumbur, Jurn. Tekhn. Fiz., 34, No.6, (1964).*
11. *I.P.Stakhanov, A.S.Stepanov, Jurn.Tekhn.Fiz., 34, 399 (1964).*
12. *B.Ya.Moijes, G.E.Pikus, Fiz. Tverd. Tela, 2, 756 (1960).*
13. *D.N.Mirlin, G.E.Pikus, V.G.Yur'ev, Jurn.Tekhn.Fiz., 32, No.6, 762 (1962).*
14. *V.P.Karmasin, I.P.Stakhanov, Jurn. Prikl. Mekh. i Tekhn. Fiz., No.5 (1963).*

317

15. *V.P.Karmasin, I.I.Kasikov, I.P.Stakhanov, Dokl. na XI Vsesoyusn. Konf. po Fiz. Osn. Katodn. Electroniki, Kiev, 1963.*

16. *H.D.Morgulis, S.M.Levitskij, I.N.Groshev, Radiotekhn. i Electronika, 7, 352 (1962).*

17. *R.L.Aamodt, L.I.Broun, B.D.Nichols, J.Appl.Phys., 33, 2080 (1962).*

18. *M.Gottlib, R.I.Zolloweg, Bull. Am. Soc., 5, 383 (1960).*

19. *S.A.Majev, I.P.Stakhanov, Dokl. na XI Vsesoyusn. Knof. po Fiz. Osn. Katodn. Electroniki, Kiev, 1963.*

20. *S.A.Majev, Teplofiz. Vis. Temp. (to be published). R.Ya.Kucherov, L.E.Rikenglaz, Jurn.Tekhn.Fiz., 37, 125 (1959).*

21. *M.A.Lebedev, Jurn.Tekhn.Fiz. (to be published).*

22. *Yu.K.Gus'kov, M.A.Lebedev, I.P.Stakhanov, Dokl. na XI Vsesoyusn. Konf. po Fiz. Osn. Katodn. Electroniki, Kiev, 1963.*

23. *G.E.Pikus, Jurn.Tekhn.Fiz., 31, 1014 (1961).*

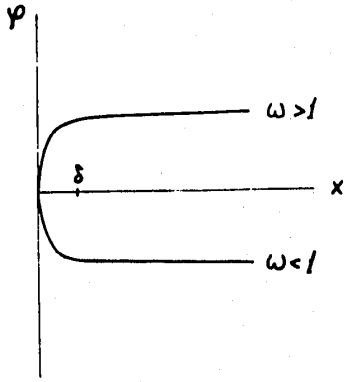

FIG.1. SCHEMATICAL POTENTIAL DISTRIBUTION NEAR A CATHODE; δ IS DEBAY RADIUS.

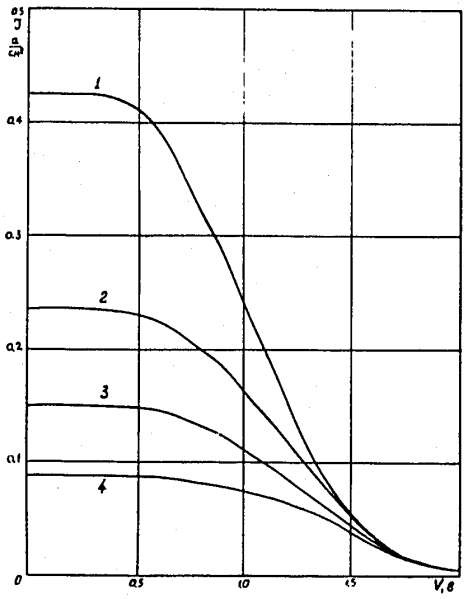

FIG.2. THE NUBERAL CALCULATIONS OF THE VOLTAGE-CURRENT CHARACTERISTICS AT T'=1800°K, T''=700°K, p=1.86 mm Hg, L=1mm.
(1) W'=2.15–2.80ev; (2) W'=3.1ev; (3) W'=3.2ev; (4) W'=3.3ev.

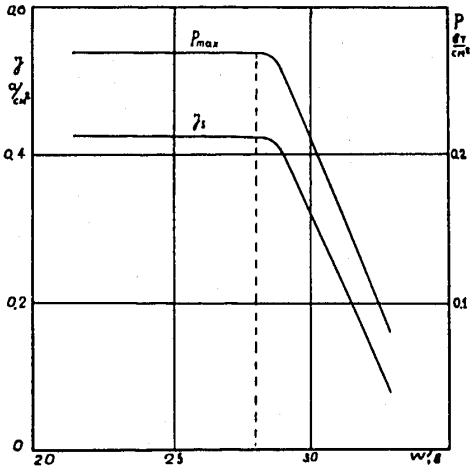

FIG.3. I_s AND P_{max} vs CATHODE WORK FUNCTION W'. THE PLASMA CHEMICAL POTENTIAL EQUALS TO 2.80EV; T'=1800°K; T''=700°K; L=1 mm; p=1.86 mm Hg.

317

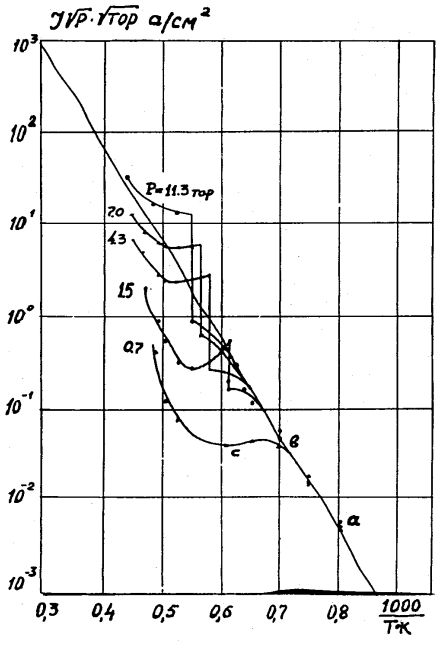

FIG.4. I_s IS THE SHORT-CIRCUIT CURRENT; L=0.7 mm; NIOBIUM CATHODE.

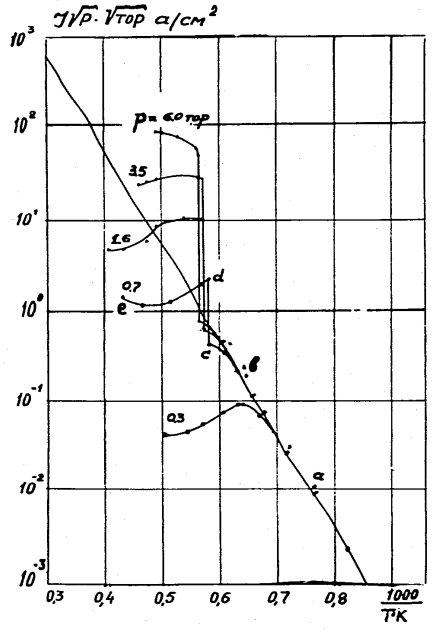

FIG.5. I_s IS THE SHORT-CIRCUIT CURRENT; L=0.7 mm; RHENIUM CATHODE.

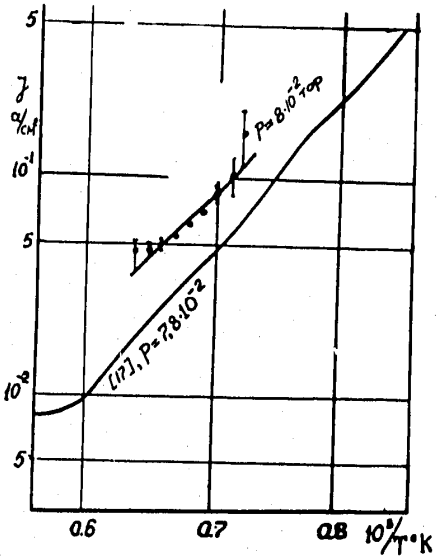

FIG.6. THE COMPARISON OF EMISSION CURRENTS FROM MOLYBDENUM IN Cs VAPOUR OBTAINED BY VARIOUS METHODS.

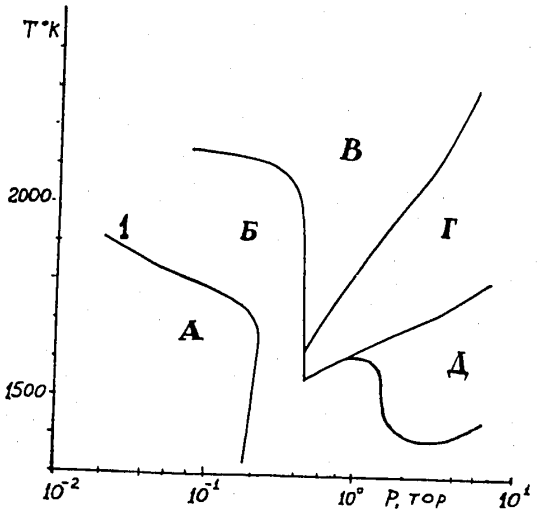

FIG.7. THE EXPERIMENTAL LIMITS OF OPERATION REGIMES OF THE CONVERTER WITH Mo CATHODE; L=0.5 mm. THE REGION "А" CORRESPONDS TO THE QUASI-VACUUM REGIME. CURVE I IS L=1. THE REGION "Б" CORRESPONDS TO THE DIFFUSION REGIME. THE REGIONS "В", "Г", "Д" CORRESPOND TO THE ARC REGIME.

317

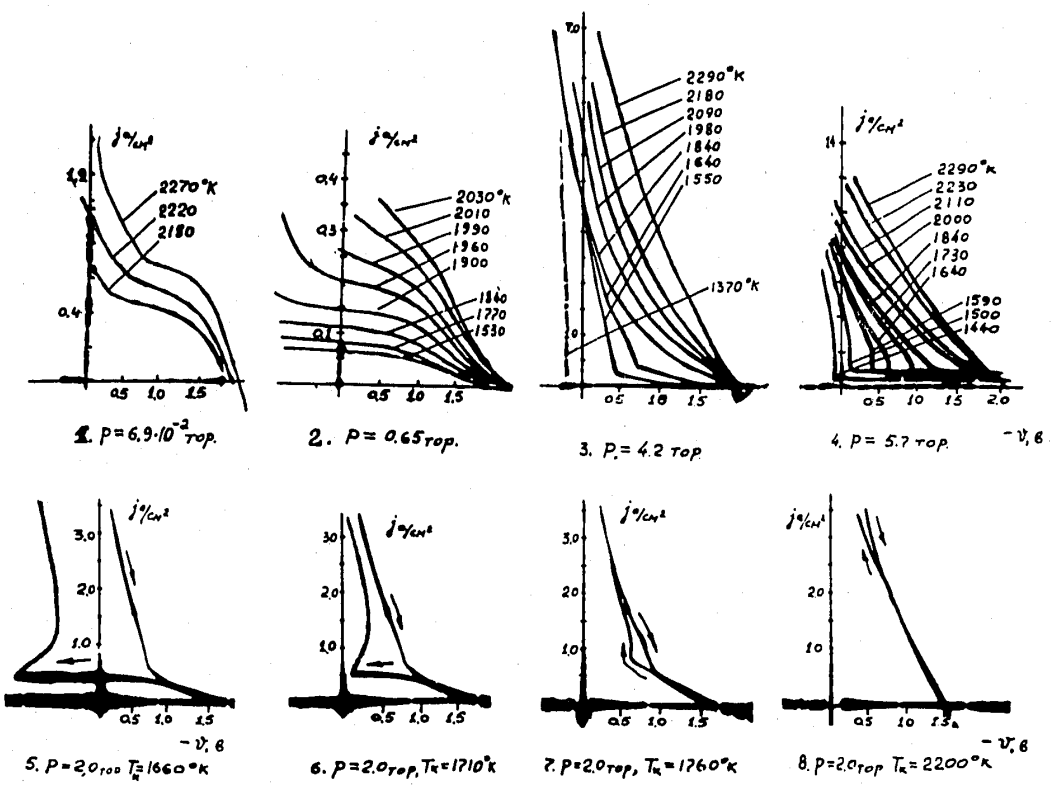

FIG.8. THE OSCILLOGRAMS OF THE V'OLTAGE-CURRENT CHARACTERISTICS IN THE ARC REGIME; L=0.7 mm.

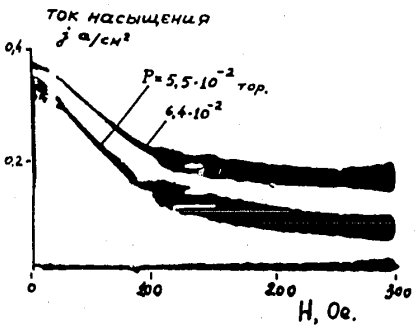

FIG.9. THE SHORT-CIRCUIT CURRENT VS MAGNETIC FIELD; MOLYBDENUM CATHODE; L=1 mm, T'=2110°K.

317

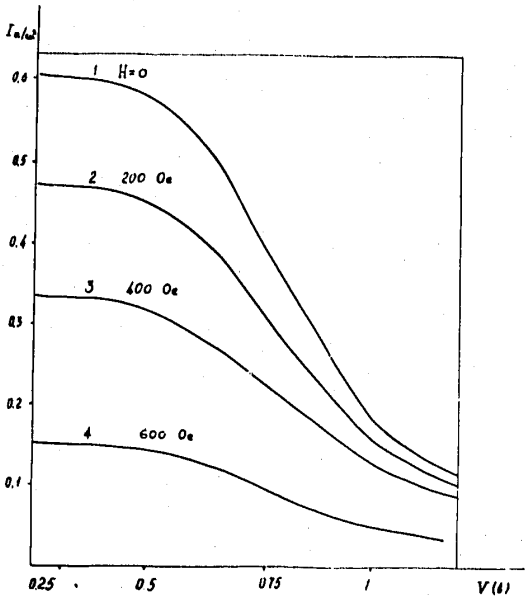

FIG.10. EFFECT OF THE TRANSVERSE MAGNETIC FIELD ON VOLTAGE-CURRENT CHARACTERISTICS; T'=1700°K; T''=800°K; p=1mm Hg; L=0.5. m; W'=2.5ev.

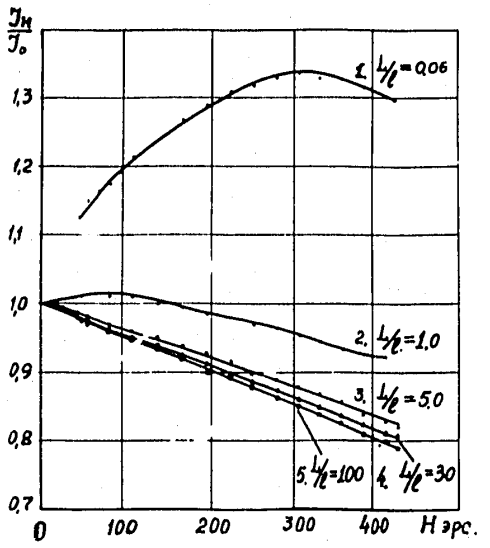

FIG.11. RELATIVE CURRENT OF A LOW-VOLTAGE ARC VS LONGITUDINAL MAGNETIC FIELD. THE BURNING POTENTIAL: (1) –5.4; (2)–2.6; (3) – 1.4; (4)–1.4; (5)–2.4 VOLT.

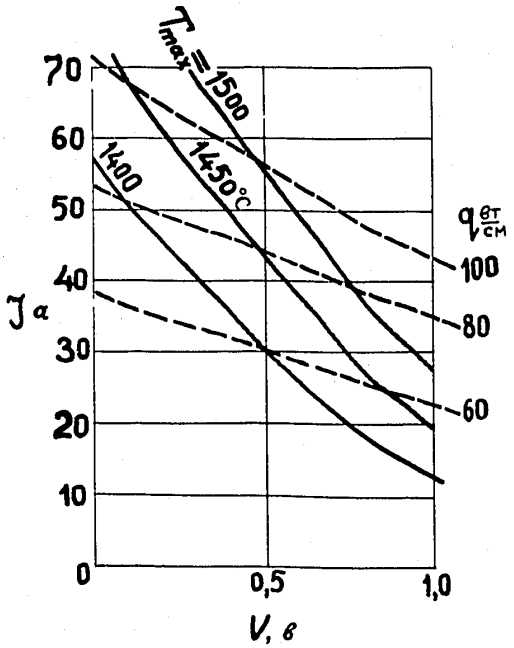

FIG.12. THE CALCULATED VOLTAGE-CURRENT CHARACTERISTICS AT VARIOUS ENERGY RELEASE DENSITIES IN A CORE. THE CATHODE SURFACE IS 15 cm^2.

317

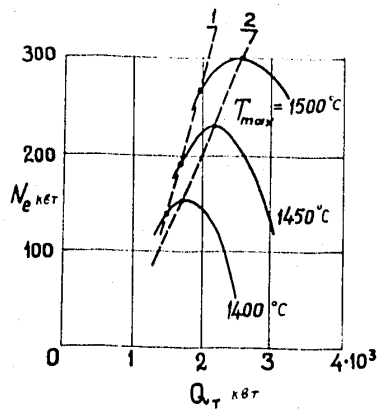

FIG.13. THE ELECTRIC POWER Ne OF THE REACTOR-CONVERTER VS THE THERMAL POWER Q_T. THE ACTIVE CORE VOLUME IS 100 LITRE, T_{max} IS THE CATHODE MAXIMUM TEMPERATURE. CURVE 1 CORRESPONDS TO THE MAXIMUM EFFICIENCY REGIME, CURVE 2 IS THE MAXIMUM POWER REGIME.

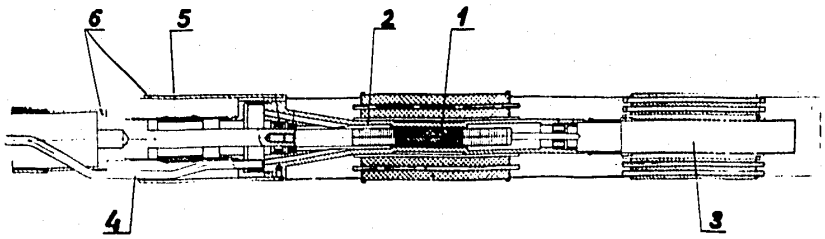

FIG.14. THE CONVERTER AMPULE WITH THE CESIUM THERMOSTAT:
1 – fuel element core; 2 – anode; 3 – cesium thermostat; 4 – vacuum pipe;
5 – isolator; 6 – current-carrying bars.

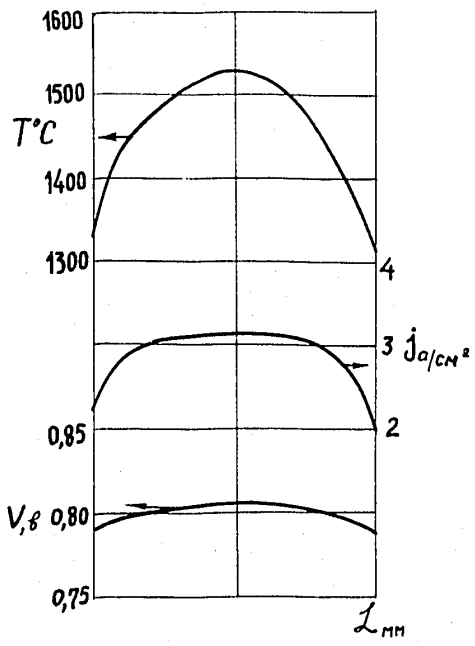

FIG.15. I, V, T, DISTRIBUTIONS ALONG THE CONVERTER. THE ENERGY RELEASE DENSITY IN A CORE IS 90 w/cm³.

317

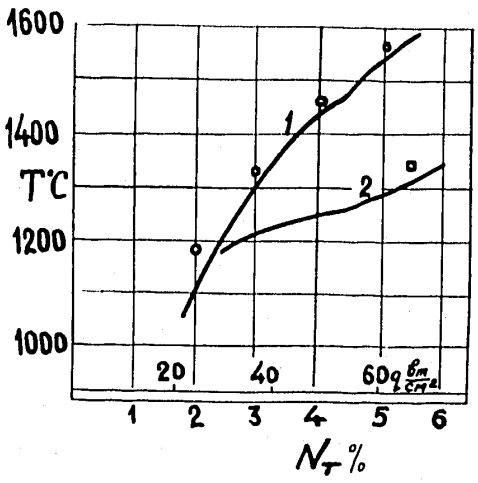

FIG.16. THE CATHODE TEMPERATURE VS THE CONVERTER THERMAL POWER; q IS CORE ENERGY RELEASE DENSITY, N_T IS THE REACTOR POWER.

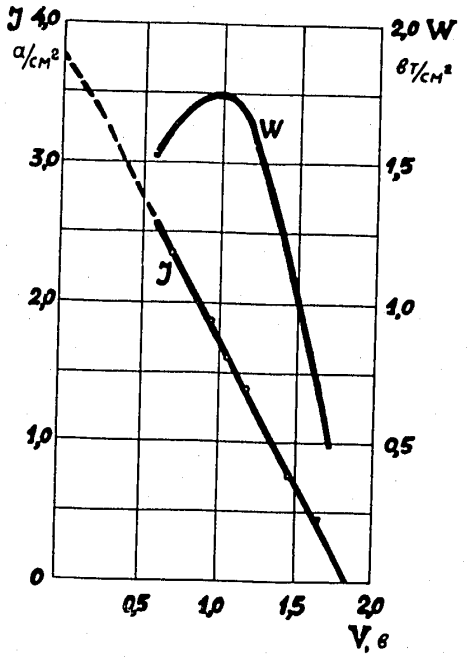

FIG.17. THE VOLTAGE-CURRENT CHARACTERISTIC AND THE OUTPUT POWER FOR THE CONVERTER WITH Mo CATHODE; T'=1600°C.

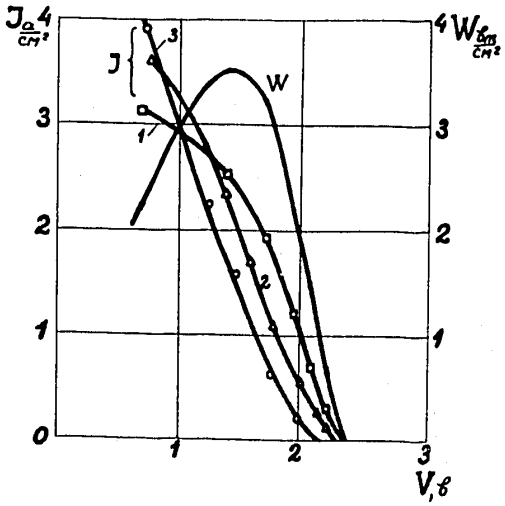

FIG.18. THE VOLTAGE-CURRENT CHARACTERISTIC AND THE OUTPUT POWER FOR THE CONVERTER WITH UC–ZrC CATHODE; T'=1500°C; (1) p=0.15; (2) p=0.2; (3) p=4 mm Hg

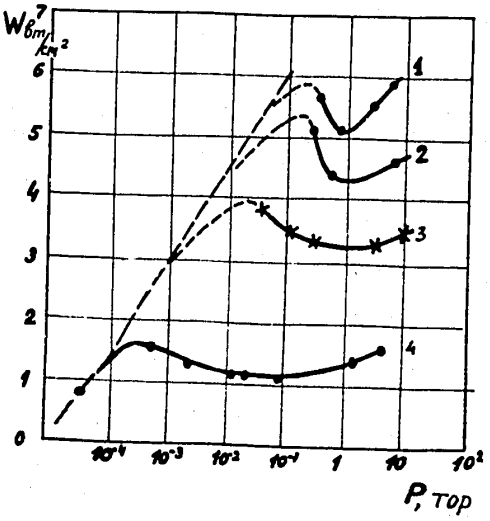

FIG.19. THE OUTPUT POWER OF THE CONVERTER WITH UC–ZrC CATHODE VS CESIUM PRESSURE; (1) T'=1600°C; (2) T'=1550°C; (3) T'=1500°C; (4) T'=1250°C.